PNAS
www.pnas.org

Supplementary Information

Stimuli-responsive composite biopolymer actuators with selective spatial deformation behavior

Yushu Wang, Wenwen Huang, Yu Wang, Xuan Mu, Shengjie Ling, Haipeng Yu, Wenshuai Chen, Chengchen Guo, Matthew C. Watson, Yingjie Yu, Lauren D. Black III, Meng Li, Fiorenzo G. Omenetto, Chunmei Li and David L. Kaplan

Corresponding author: david.kaplan@tufts.edu; chunmei.li@tufts.edu

This PDF file includes:

Supplementary text
Figures S1 to S18
Legends for Movies S1

Other supplementary materials for this manuscript include the following:

Movies S1.

www.pnas.org/cgi/doi/10.1073/pnas.2002996117

Supplementary Information

Material Characterization:

Differential Scanning Calorimetry: DSC measurements were performed with Nano DSC II Model 6100 (Calorimetry Sciences Corp., Lindon, UT). The well-mixed SELP: HRP: H_2O_2 solutions were pipetted into the DSC sample chamber and allowed to gel at 4°C before measurement. To test the inverse transition temperature of the SELP hydrogels, the SELP hydrogels were equilibrated for 30 min, and then heated in the sample chamber from 0 to 100°C at a rate of 2°C min^{-1} and cooled to 0°C at the same rate. The same volume of solvent was placed in the reference chamber during each scan. The baseline scans were taken with the solvent under the same condition and subtracted from the sample scans.

Mechanical Tests: DMA studies were processed on a TA Instruments RSA3 dynamic mechanical analyzer (TA Instruments, New Castle, DE) with RSA-G2 immersion system. Cylindrical SELP hydrogels, ~9 mm in diameter and 4 mm in thickness, were submerged in DI water or NaCl solutions in the RSA-G2 solvent cup during DMA measurements. The storage modulus, E′, which is related to the elastic deformation, and the loss modulus, E ″, which is related to the viscous deformation and energy absorption, were determined. To assess the viscoelastic properties of the SELP hydrogels, dynamic single point tests at a strain of 5%, with 1.0 Hz, were performed at 4, 37 and 60°C with an equilibrium time of 30 min per step. The mechanical properties of the wet CNF membranes were evaluated by a universal tensile tester (Instron Model 3366, MA) with a 100 N load cell and a 2 mm min^{-1} of speed at room temperature. The CNF membranes were fixed in a

clamp and then stretched to break. Contraction force of the SELP hydrogels was measured using a force transducer. Ring-shape hydrogels with inner diameter of 6 mm were placed in a NaCl bath at room temperature, and looped around the force transducer cantilever and a stationary post. Data were acquired using a previously designed custom-made LabVIEW virtual instrument (National Instruments Corporation). Briefly, contraction force outputs were received via a NI-DAQ, were read and recorded on screen and written to a text file. Force measurements were sampled at 1000 Hz and recorded for over one hour for each sample. Each measurement was run at least three times.

Scanning Electron Microscopy: Scanning Electron Microscopy images were captured using a Zeiss Ultra55 SEM in the Center for Nanoscale Systems at Harvard University. SELP hydrogels and of the SELP/CNF bilayer actuators were fast frozen by liquid nitrogen, freeze-dried, fractured to expose the cross-sections, and sputter coated with Pt/Pd for SEM observation.

Fourier Transform Infrared Spectroscopy: The chemical structure of the SELP hydrogels were recorded by a FTIR-6200 (Jasco Instruments, Easton, MD) spectrometer. ATR-FTIR was performed with a horizontal MIRacle™ attenuated total reflection attachment (Madison, WI). Data was obtained by averaging 32 scans with a resolution of 4 cm^{-1} within the wavenumber range of 600 and 4000 cm^{-1}. The background spectra were taken under the same conditions and subtracted from the media scans.

Deswelling and reversible Properties of SELP hydrogels: To evaluate the stimuli-responsive properties, all the SELP hydrogels were initially equilibrated in

DI water at 4°C. Then the hydrogels were equilibrated in an aqueous environment such as DI water (at 37°C or 60°C), in a series of concentrations of NaCl solutions (at room temperature) and in 500 mM NaCl solution (at room temperature and 37°C), respectively. The equilibrium deswelling ratios of the SELP hydrogels were calculated by:

$$\text{Deswelling ratio} = (1-W_{deswelling} / W_{original}) \times 100\% \quad (1)$$

where $W_{deswelling}$ and $W_{original}$ are the weight of the SELP hydrogels under specific environment stimulus and the weight of the hydrogel equilibrated in DI water at 4°C. To monitor the reversibility of the SELP hydrogels, the deswelling hydrogels were equilibrated in DI water at 4°C before the next cyclic test.

Actuation Processing of SELP/CNFs: For SELP/CNF actuators with various 3D origami-like geometries, when those actuators achieved maximum deformation in the NaCl solution at room temperature, they were taken out from the NaCl solution and photographed. All SELP/CNF actuators were transferred from the solution to air carefully to keep their shapes unchanged as much as possible. All deformation experiments of SELP/CNF bilayer strip actuators under specific stimuli were carried out in 24-well plates. The size changes of SELP/CNF strip actuators were recorded by microscopy (OLYMPUS, SZX 9) with a digital camera (SONY, NEX-5) and analyzed with Image J. The MDC was calculated by

$$MDC = (1- D_{deformation} / L_{SELP/CNF}) \times 100\% \quad (2)$$

where $L_{SELP/CNF}$ and $D_{deformation}$ are the size of equilibrium length and the minimum inner diameters of SELP/CNF strip actuators, respectively, before and after incubating under specific stimuli. For the reversible experiments, the deformable

SELP/CNF strip actuators were equilibrated in DI water at 4°C before the next cyclic actuation. The area ratio of the petal-shaped bilayer structure was calculated by

SELP/CNF Area Ratio = A_{SELP} / A_{CNF} ..... (3)

where A_{SELP} and A_{CNF} are the area of the SELP hydrogels and the area of the excircle of the petal-shaped CNF membranes, respectively.

Finite element simulations analysis: Finite element simulations (FEA, solid mechanics module with the hygroscopic feature, COMSOL Multiphysics, 5.4, Burlington, MA) were used to investigate the shape morphing process of the assembled SELP/CNF actuators. The 3D FEA model was established according to the actual configuration (6 stacked layers) and geometry of the SELP/CNF actuators (Figure 4). We assumed both CNF membranes and SELP hydrogels were hyperelastic materials and modeled the salt-induced strain by the equation of hygroscopic swelling, $\varepsilon=\beta \bullet \Delta C$, where ε is the strain, β is the coefficient derived from Figure 2b, and ΔC is the concentration of NaCl.

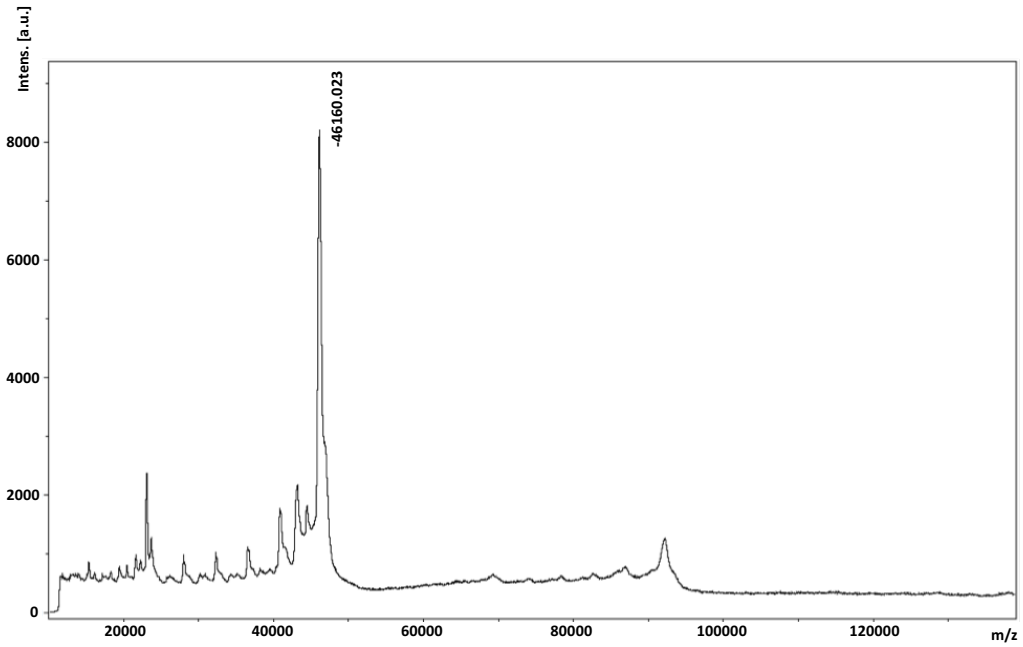

Fig. S1. MALDI-TOF analysis of SELP.

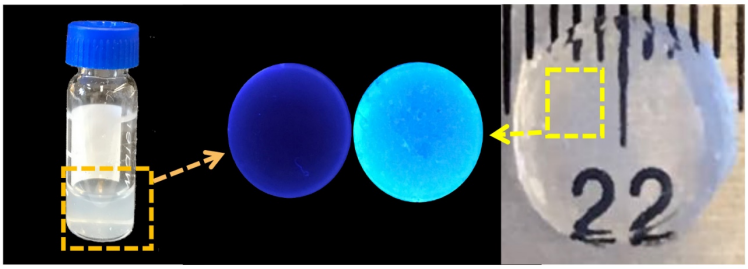

Fig. S2. The optical images of SELP solution and SELP hydrogels. In contrast to the SELP solution, the cross-linked hydrogel presents blue fluorescence when irradiated under UV due to the formation of di-tyrosine bonds. The background of the photograph is a ruler and each small grid represents 1 mm.

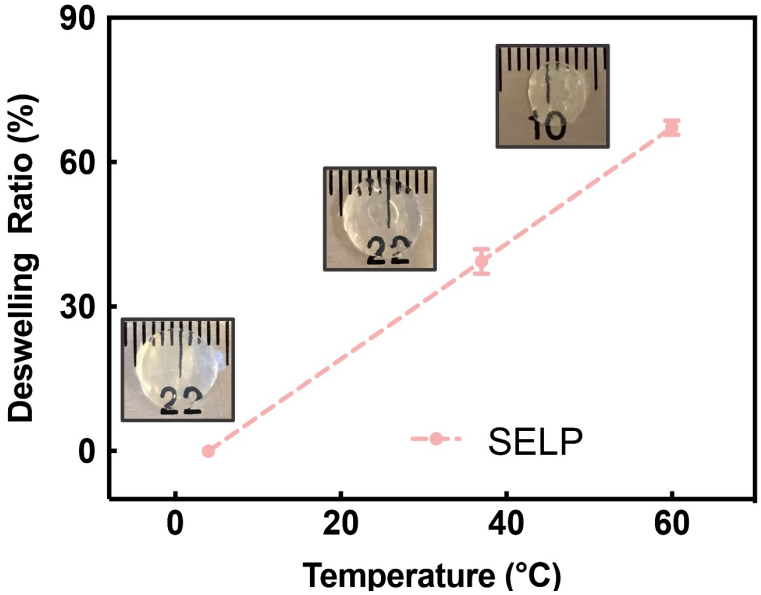

Fig. S3. Deswelling ratios of the SELP hydrogels under temperature stimuli. The inserts are photographs of the same SELP hydrogels in DI water at temperatures of 4, 37 and 60°C. The background of each photograph is a ruler and each small grid represents 1 mm.

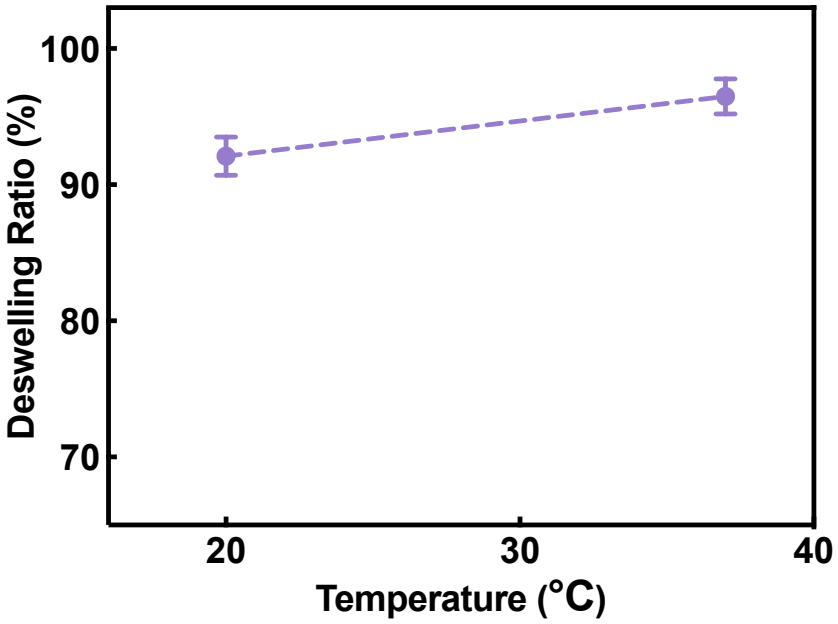

Fig. S4. Deswelling ratio versus temperature curve of the SELP hydrogels immersed in 500 mM NaCl.

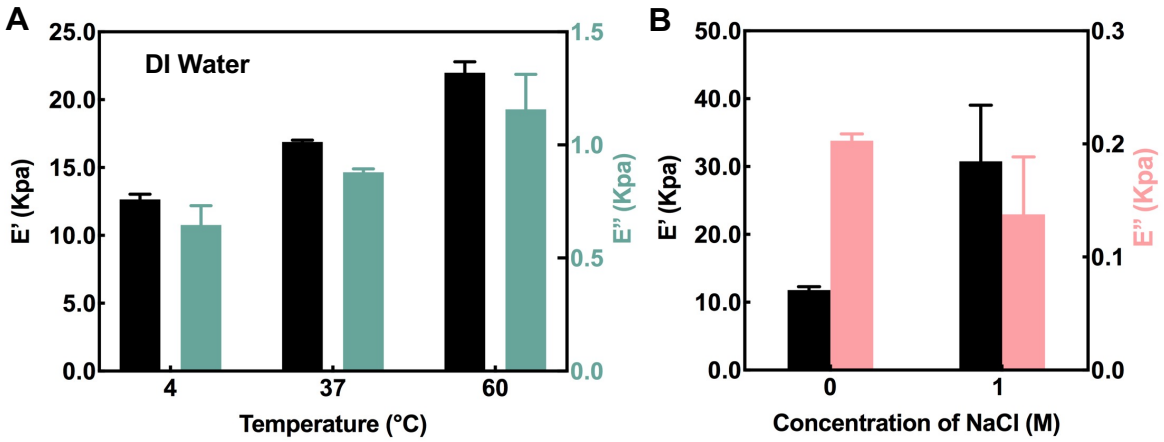

Fig. S5. Storage modulus (E') and modulus loss (E'') of SELP hydrogels were determined by DMA in (A) DI water at 4, 37 and 60°C and (B) 1M NaCl at room temperature.

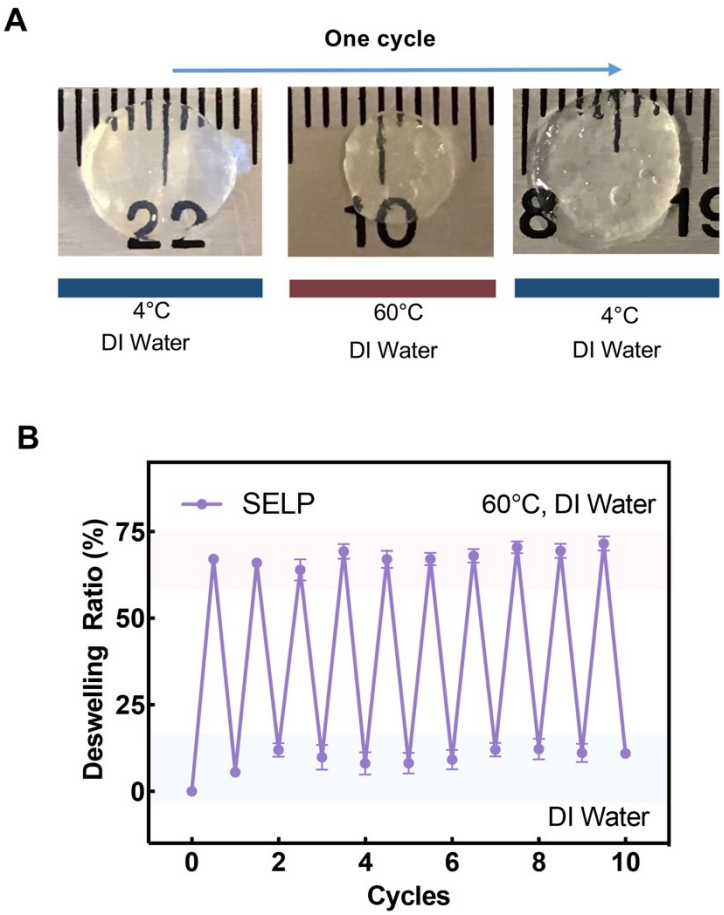

Fig. S6. (A) Photographs of the SELP hydrogels in DI water at temperatures of 4, 60°C and further equilibrated back to 4°C. The background of each photograph is a ruler and each small grid represents 1 mm. (B) Cyclic stability of the deswelling ratios of the SELP hydrogels in DI water triggered by temperature changes between 4°C to 60°C.

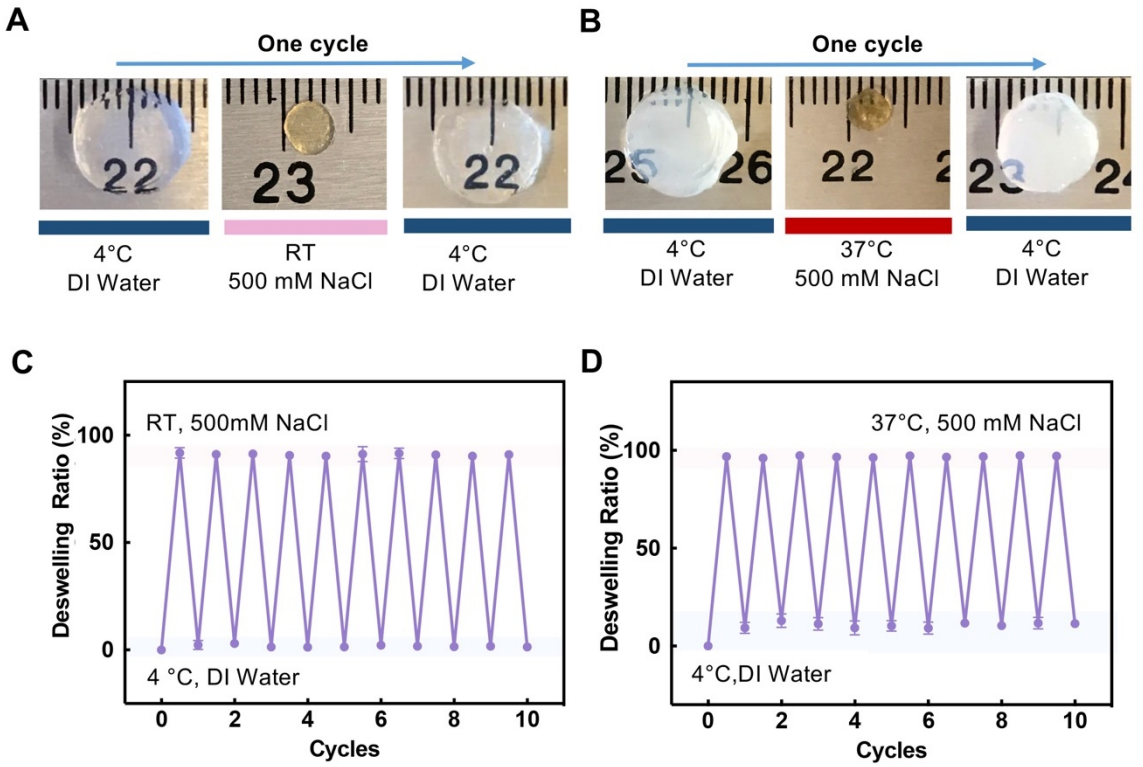

Fig. S7. (A) Photographs of the original SELP hydrogels in DI water at 4°C, 500 mM NaCl solution at room temperature and further equilibrated back in DI water at 4°C. (B) Photographs of the original SELP hydrogels in DI water at 4°C, 500 mM NaCl solution at 37°C and further equilibrated back in DI water at 4°C. The background of each photograph is a ruler and each small grid represents 1 mm. (C, D) Cyclic actuating process of the deswelling ratios of the SELP hydrogels triggered by the same conditions as (A, B) respectively.

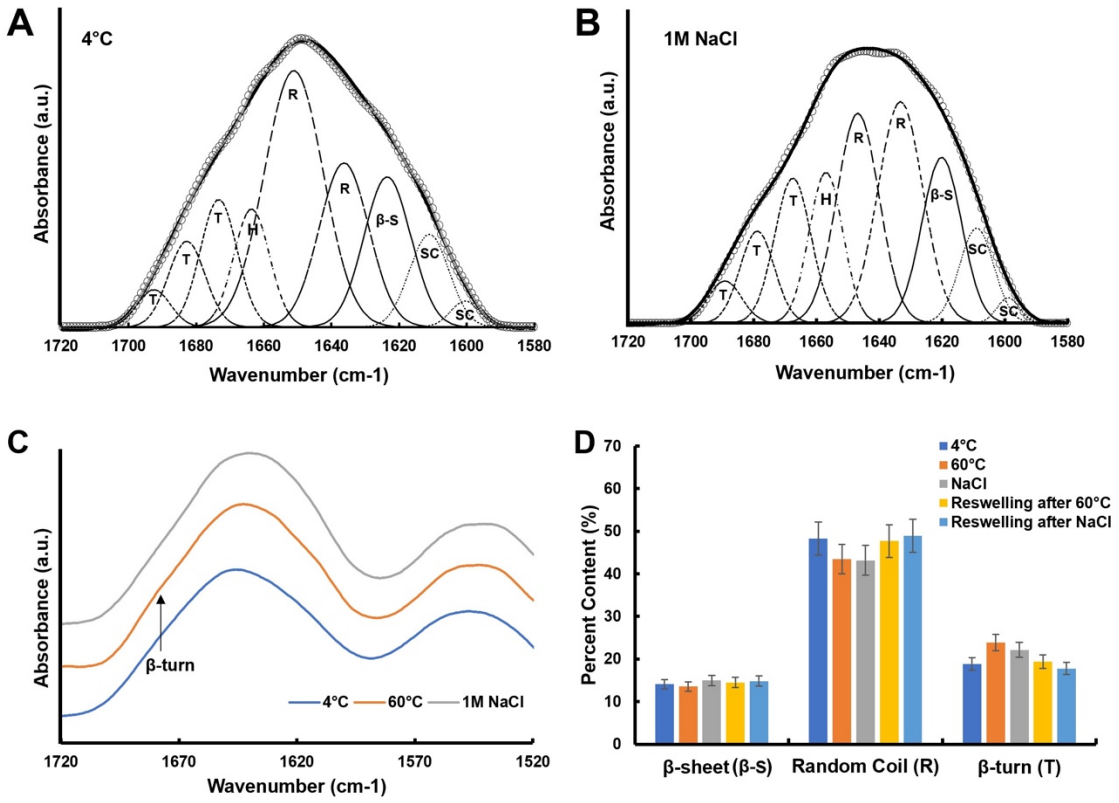

Fig. S8. FTIR analysis of SELP hydrogels. Fourier self-deconvolution of amide I spectra of SELP hydrogel in (A) DI water at 4°C and (B) 1M NaCl solution. Open circles - summation of Gaussian peaks; heavy line - measured data; thin solid and dashed lines -- individual Gaussian peaks; bands are marked as random coil (R), β-sheets (β-S), alpha-helices (H), β-turns (T), and side chains (SC). (C) FTIR absorbance spectra of SELP hydrogels under various conditions. (D) Calculated percentages of secondary structures for SELP hydrogels under various conditions.

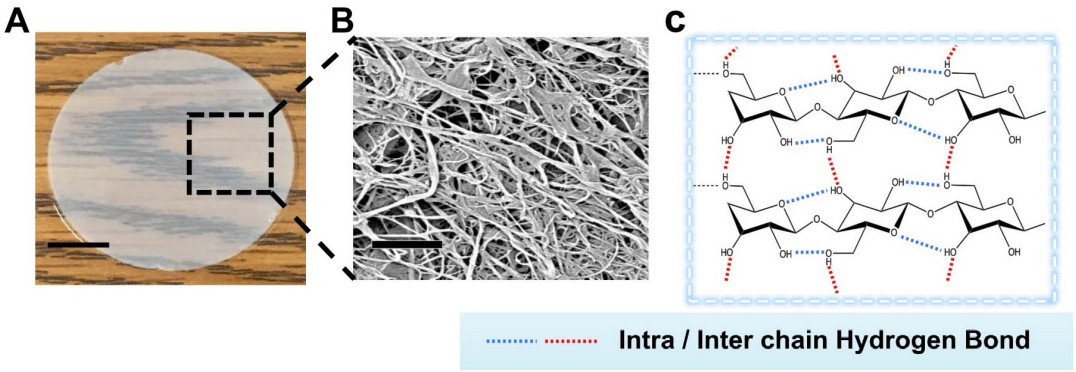

Fig. S9. (A) Photograph and (B) SEM of the CNF membrane. (C) Chemical formula of cellulose. Scale bar in (A) and (B) are 1 cm and 2 μm, respectively.

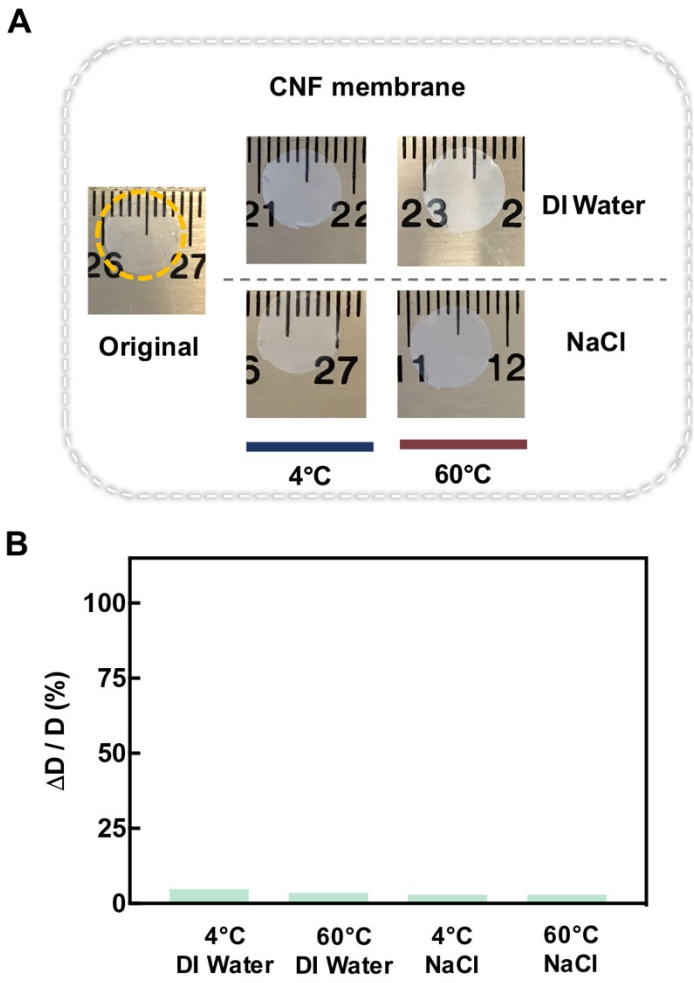

Fig. S10. (A) Photographs of the CNF membranes immersed in DI water and 1M NaCl solution at 4 and 60°C. The background of each photograph is a ruler and each small grid represents 1 mm. (B) Diameter stability of the CNF membranes diameter changes under these stimuli related to the original sizes.

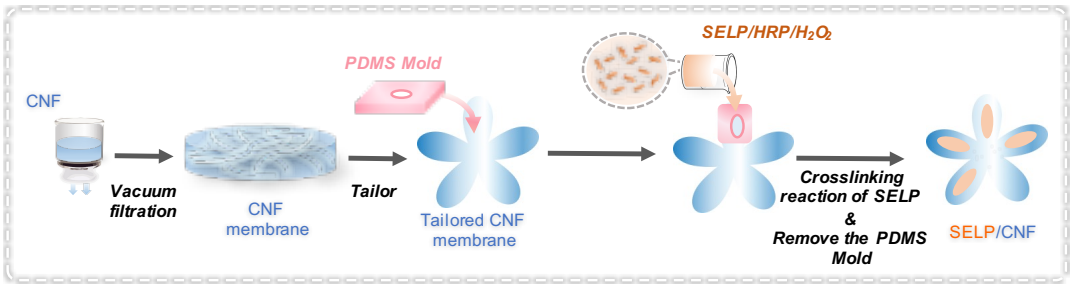

Fig. S11. Schematic of the fabrication of the site-selective SELP/CNF actuators.

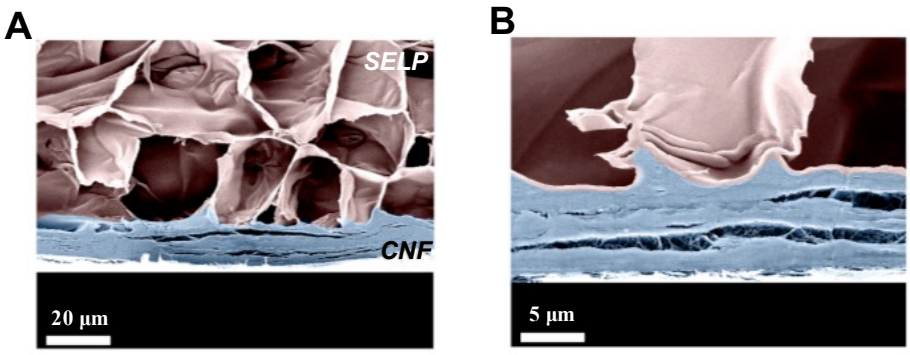

Fig. S12. (A, B) Cross-section SEM image of the SELP/CNF bilayer actuator.

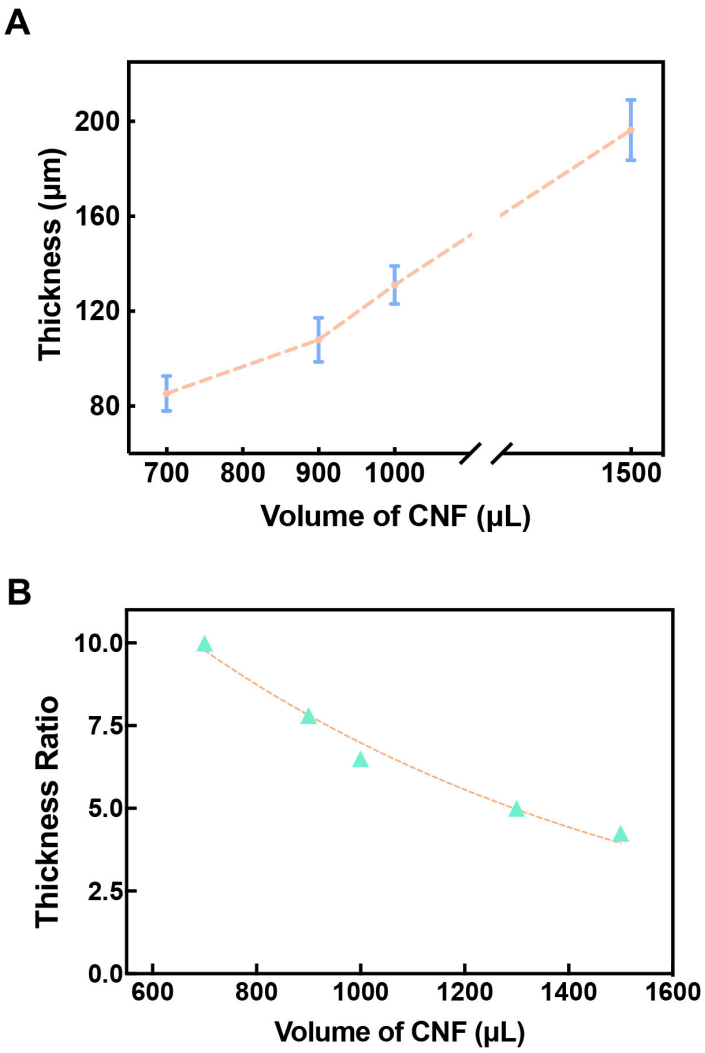

Fig. S13. (A) CNF membrane thickness versus the volume of the CNF dispersion for vacuum filtration. (B) Thickness ratio curve of the SELP hydrogel layers crosslinked by the consistent volume of 250 μL SELP: HRP: H_2O_2 solutions and the CNF layers vacuum filtrated by various volumes of CNF suspensions.

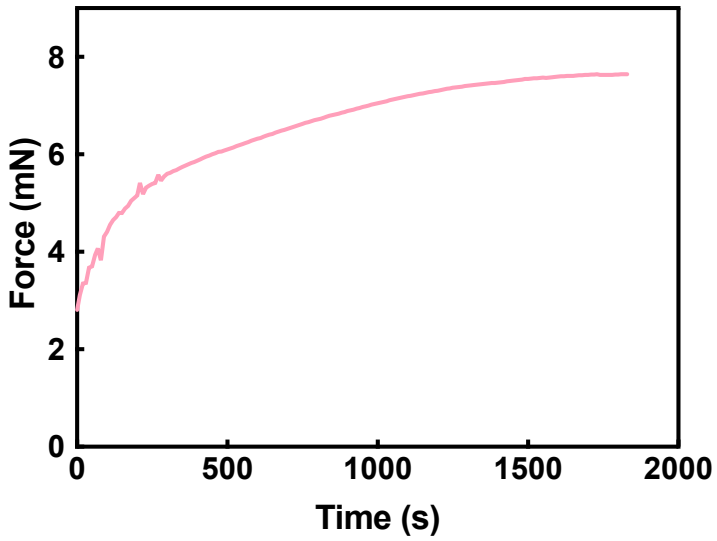

Fig. S14. Contraction force measurement of SELP hydrogel in 500 mM NaCl solution at room temperature with an average maximum contraction force of 7 mN.

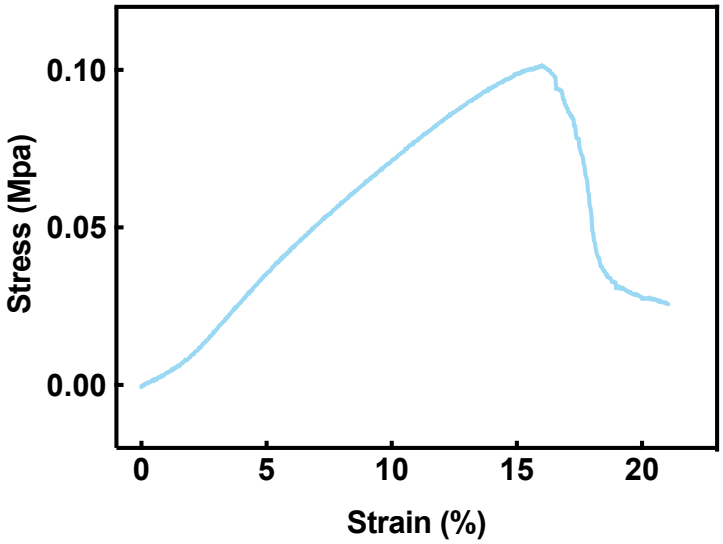

Fig. S15. Stress-strain curve of the CNF membrane during tensile testing.

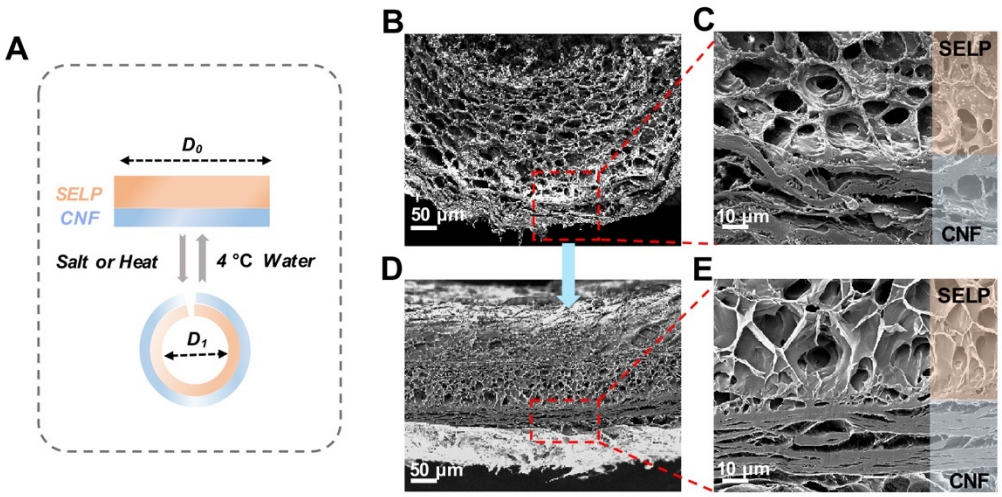

Fig. S16. (A) Schematic illustration of the reversible MDC of the bending SELP/CNF strip actuators triggered under the temperature and ionic strength stimuli and equilibrated back in DI water at 4°C. (B, C) Cross-section interface and the enlarged SEM images of the bilayer strip actuator immersed in the 500 mM NaCl solution at room temperature respectively. (D, E) Cross-section interface and the enlarged SEM images of the bilayer strip actuator equilibrated back in DI water at 4°C, respectively.

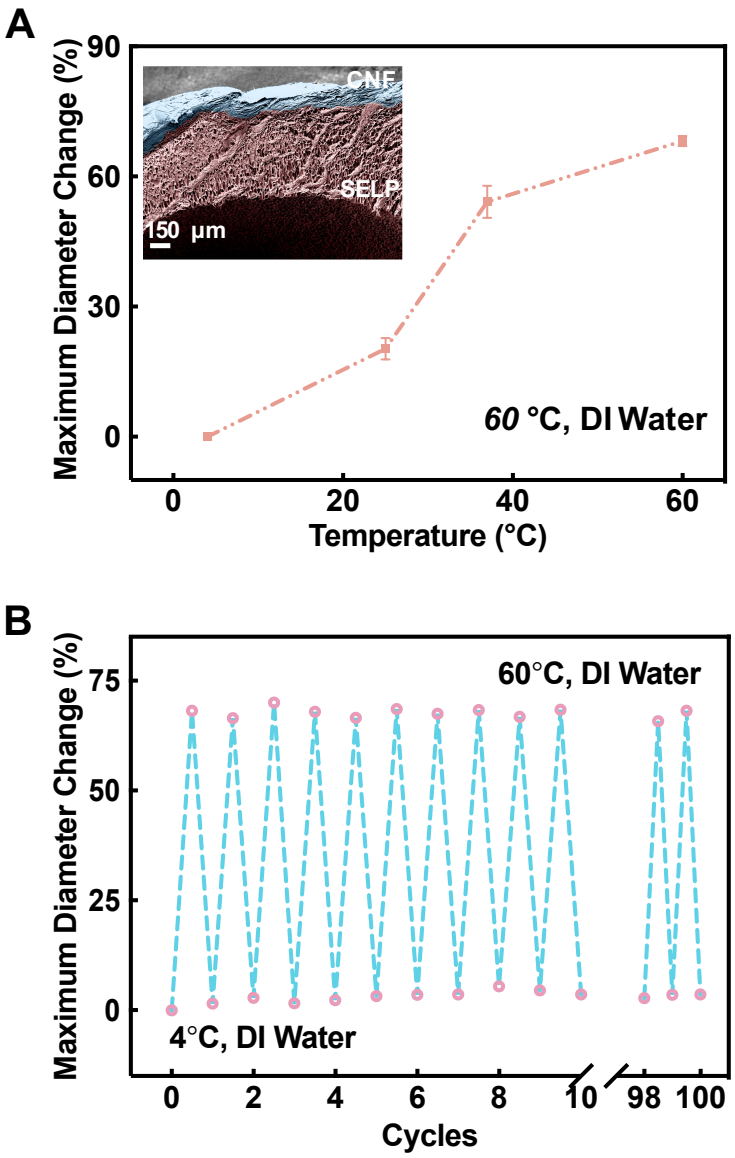

Fig. S17. (A) MDC versus temperature curves of bilayer SELP/CNF strip actuators with thickness ratios of 10 in response to temperature in DI water, the inset is SEM image of the bilayer strip actuator immersed in DI water at 60°C. (B) Cyclic stability of the MDC of the bilayer strip actuators with thickness ratio of 10 in DI water under the temperature changes from 4°C to 60°C.

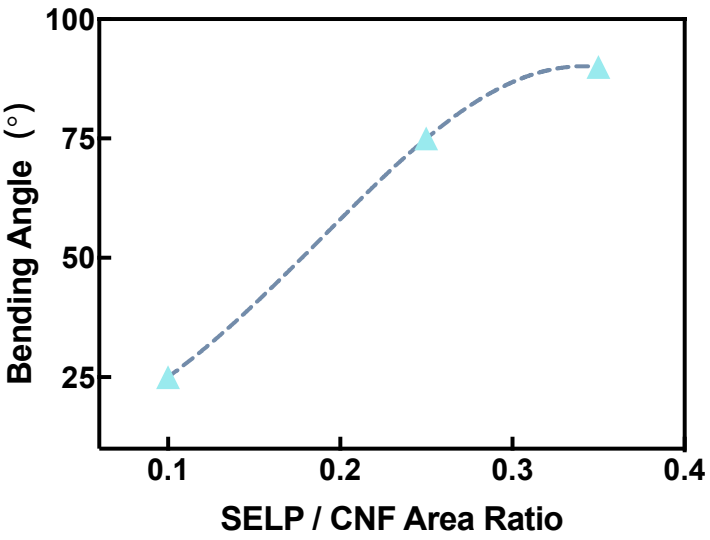

Fig. S18. Bending angles of the SELP/CNF actuators depending on the area ratios of the passive domain (CNF membrane) covered by the active domain (SELP hydrogel).

Supplementary Movies

Movie S1. The transformation process of the petal-shaped multilayer SELP/CNF actuators over time in 1M NaCl solutions at room temperature. The color of actuators was stained by water-proof inks.